THE ANNALS OF "DUNAREA DE JOS" UNIVERSITY OF GALATI.
FASCICLE IX. METALLURGY AND MATERIALS SCIENCE
N$^0$. 2 – 2012, ISSN 1453 – 083X

# STUDY FOR EVALUATION AND OPTIMIZATION OF MINERAL COMPOSITION AND STRUCTURE OF IRON ORE GRANULATION IN SINTERING PROCESS

**Paul Petruș MOGOȘ, Nicolae CONSTANTIN, Sinziana ITTU, Denisa-Elena ANCA, Lavinia-Marilena HARCEA**
"Polytechnic" University of Bucharest,
email: mogospaul@yahoo.com

## ABSTRACT

*The characterization of iron ore particles is of vital importance for the study of mineral composition. The specific surface area of iron ore particles can be measured by laser diffraction, and mathematical models (based on the size distribution). Particle size fractions and chemical composition were determined of several types of iron ore (symbolically marked A, B, C, D, E, F). These features have direct influence on the sintering process by particle size analysis, permeability, reducibility, porosity, CaO/SiO ratio, influence of MnO in sinter. The granulation experiment show that these minerals (more than 50% with diameters of <1mm) can be successfully used in the sintering process, or by alloying with other minerals in Europe. Large irregularly shaped and adhesive particles can get a higher efficiency of granulation easily. The usage of iron ore with big and rough particles can improve the permeability while the iron ore with smooth and sphere particles has poor ability of granulation.*

KEYWORDS: iron ore, sinter, size distribution, chemical composition, mathematical model

## 1. Introduction

The performance of blast furnace depends, to a greater extent, on the physical and chemical characteristics of the burden materials and their consistency. Sinter constitutes 70–80% of the iron bearing burden material in the modern blast furnaces (**Figure 1**).

An important aspect of the sinter, as ferrous burden, is that it could be tailor made. Its physical & chemical properties depend on the properties of individual components and on its micro-structure, especially on the size, shape distribution and the mutual interaction of the individual components.

A thorough appreciation of the microstructure of sinter is a basic necessity and the first step towards establishing structure–property relationship.

Sinter is an agglomerate made of fine iron ore that is cheaper than pellets and lump iron ore and is superior in terms of reducibility and dropping characteristics. For the two reasons of better production, cost performance and stable operation of blast furnaces, sinter has been used in many countries as one of the main sources for blast furnace operation.

In order to satisfy the need to improve the productivity of sinter, a broad range of research and development efforts have been made from the viewpoints of the technology to pre-treat fine iron ore and the technology to control the charging structure on the entire spread of the sintering bed.

The characterization of the particle size and the surface features of iron ores is of vital importance for the study of mineral processing. The specific surface area of iron ore particles can be measured by laser diffraction, and mathematical models based on the size distribution. However, what is the difference among these methods and what is the indication of the results were less discussed on the iron ore granulation, which is the exactly topic of the present study.

With the progressive deterioration in the quality of iron ore in recent years, there has been an increase in the quantity of pisolite ore used in the raw material mix. It is known that the use of large quantities of these ores as sinter raw materials greatly reduces the granulation and air permeability of the raw material packed bed, resulting in reduced productivity.

This is thought to be because these ores are porous and the added moisture is absorbed into the ore particles, with the result that the volume of moisture is not sufficient for granulation. Accordingly, to ensure the stable use of large quantities of these ores, it is necessary to optimize the adding volume of moisture. Accordingly, it takes a certain period to stabilize the optimal moisture value, and this was one factor in producing instability in the operations.

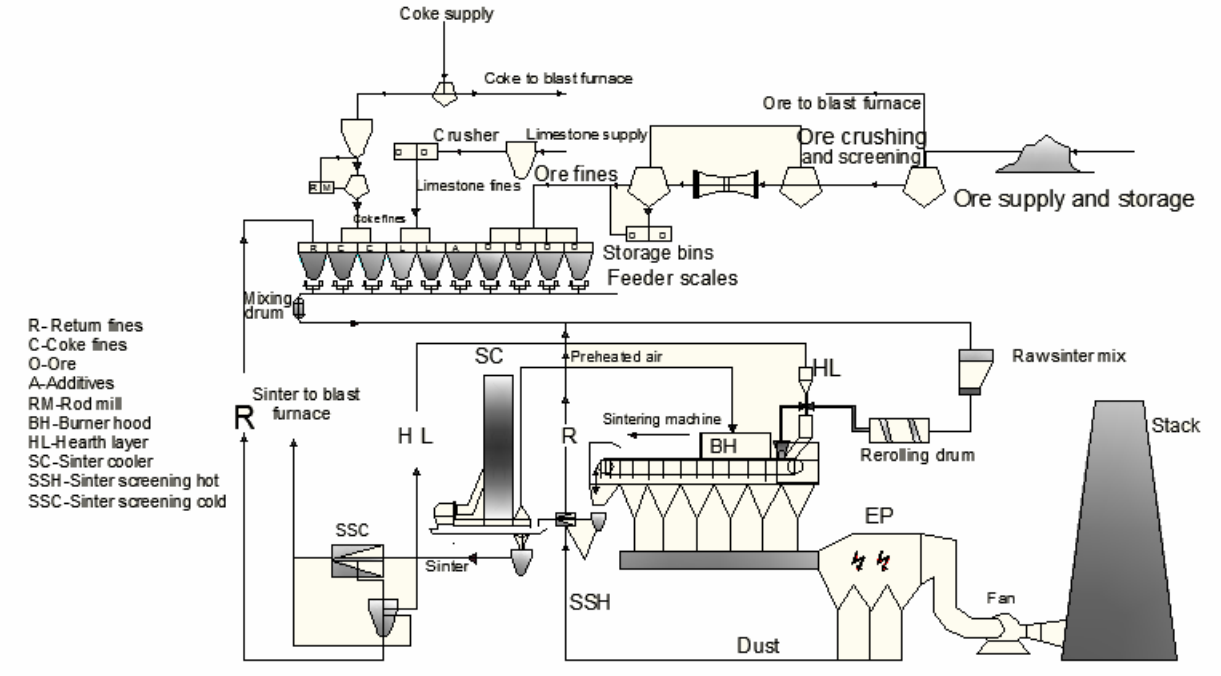


***Fig. 1**. Schematic diagram of the sintering process*

## 2. Materials and methods

The properties of iron ore sample related to granulation were measured from different locations: A, B, C, D, E, F. Diffraction shows that all are in compositions a significant amount of Fe (from 64.2% to 68.3%). Minerals present in raw materials are: goethite, hydrated iron oxide, hematite, kaolinite and quartz.

### *2.1 Particle size measurement*

***Table 1**. Particles size analysis.*

| Size (μ) | Ore A | Ore B | Ore C | Ore D | Ore E | Ore F |
|---|---|---|---|---|---|---|
| 8mm | 2 | 2 | 6 | 2 | 20 | 21 |
| 4mm | 8 | 7 | 24 | 7 | 14 | 12 |
| 2mm | 0 | 0 | 0 | 20 | 12 | 5 |
| 1mm | 31 | 48 | 26 | 30 | 12 | 9 |
| 500μm | 0 | 0 | 10 | 13 | 10 | 10 |
| 250 μm | 0 | 0 | 8 | 11 | 0 | 0 |
| 180 μm | 22 | 27 | 4 | 4 | 13 | 17 |
| 90 μm | 12 | 4 | 6 | 5 | 4 | 7 |
| 63 μm | 10 | 0 | 15 | 8 | 3 | 5 |
| -63μm | 15 | 12 | 0 | 0 | 11 | 11 |

Samples of iron ore properties related to grain are presented in **Table 1, Figure 2**, for each sample separately, using laser diffraction.

Parameters follow:
-mixture sintering;
-$CaO/SiO_2$ report.

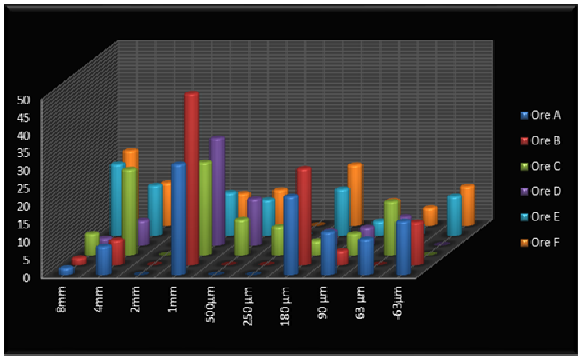


***Fig. 2**. Particle size distribution*

In the present study, six samples of iron ore were selected for the measurements. The samples were analyzed by particle size, analysis that was performed in a 0.5kg volume of each sample

determining the particle size classes between 63µm-8mm. Particle size distribution for each type of ore is presented in **Tables 2-7** and **Figure 3**.

In terms of grain, more than 50% of the particles are> 1mm, which contributes to the sintering process by high productivity and permeability. Also we observe a significant percentage of fine ore, but they may become adherent particles, increasing the diameter.

***Tables 2-7.*** *Particles size distribution*

| Size (µ) | Ore A (%) | Size (µ) | Ore B (%) |
|---|---|---|---|
| 4mm÷8mm | 2 | 4mm÷8mm | 2 |
| 2mm÷4mm | 8 | 2mm÷4mm | 7 |
| 1mm÷2mm | 0 | 1mm÷2mm | 0 |
| 500µm÷1mm | 31 | 500µm÷1mm | 48 |
| 250 µm÷500µm | 0 | 250 µm÷500µm | 0 |
| 180 µm÷250 µm | 0 | 180 µm÷250 µm | 0 |
| 90 µm÷180 µm | 22 | 90 µm÷180 µm | 27 |
| 63 µm÷90 µm | 12 | 63 µm÷90 µm | 4 |
| -63µm÷63µm | 10 | -63µm÷63µm | 0 |
| <-63 µm | 15 | <-63 µm | 12 |

| Size (µ) | Ore C (%) | Size (µ) | Ore D (%) |
|---|---|---|---|
| 4mm÷8mm | 6 | 4mm÷8mm | 2 |
| 2mm÷4mm | 24 | 2mm÷4mm | 7 |
| 1mm÷2mm | 0 | 1mm÷2mm | 20 |
| 500µm÷1mm | 26 | 500µm÷1mm | 30 |
| 250 µm÷500µm | 10 | 250 µm÷500µm | 13 |
| 180 µm÷250 µm | 8 | 180 µm÷250 µm | 11 |
| 90 µm÷180 µm | 4 | 90 µm÷180 µm | 4 |
| 63 µm÷90 µm | 6 | 63 µm÷90 µm | 5 |
| -63µm÷63µm | 15 | -63µm÷63µm | 8 |
| <-63 µm | 0 | <-63 µm | 0 |

| Size (µ) | Ore E (%) | Size (µ) | Ore F (%) |
|---|---|---|---|
| 4mm÷8mm | 20 | 4mm÷8mm | 21 |
| 2mm÷4mm | 14 | 2mm÷4mm | 12 |
| 1mm÷2mm | 12 | 1mm÷2mm | 5 |
| 500µm÷1mm | 12 | 500µm÷1mm | 9 |
| 250 µm÷500µm | 10 | 250 µm÷500µm | 10 |
| 180 µm÷250 µm | 0 | 180 µm÷250 µm | 0 |
| 90 µm÷180 µm | 13 | 90 µm÷180 µm | 17 |
| 63 µm÷90 µm | 4 | 63 µm÷90 µm | 7 |
| -63µm÷63µm | 3 | -63µm÷63µm | 5 |
| <-63 µm | 11 | <-63 µm | 11 |

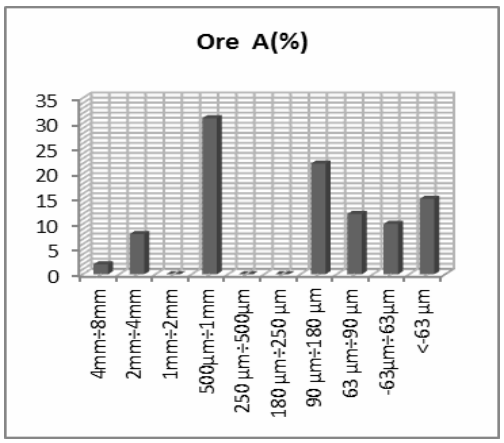


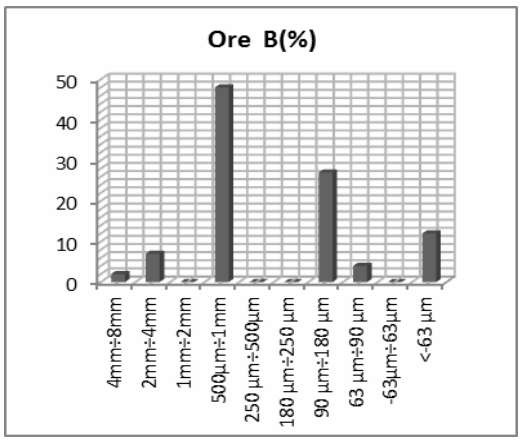


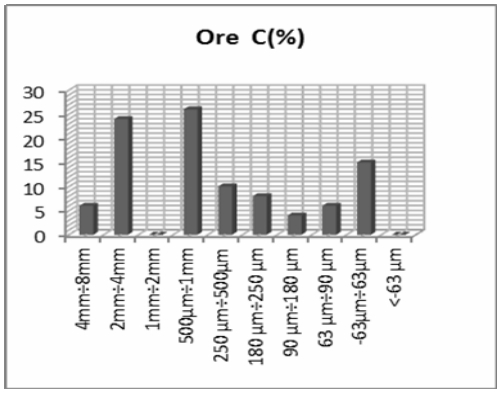


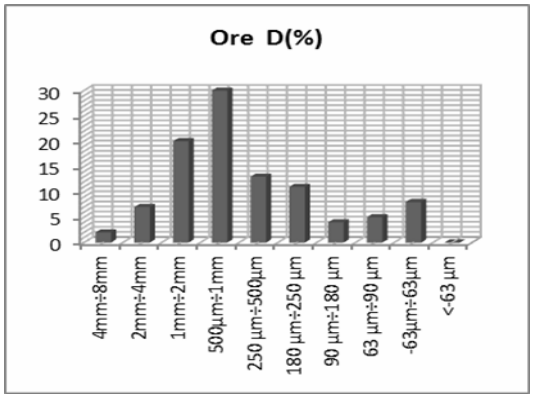

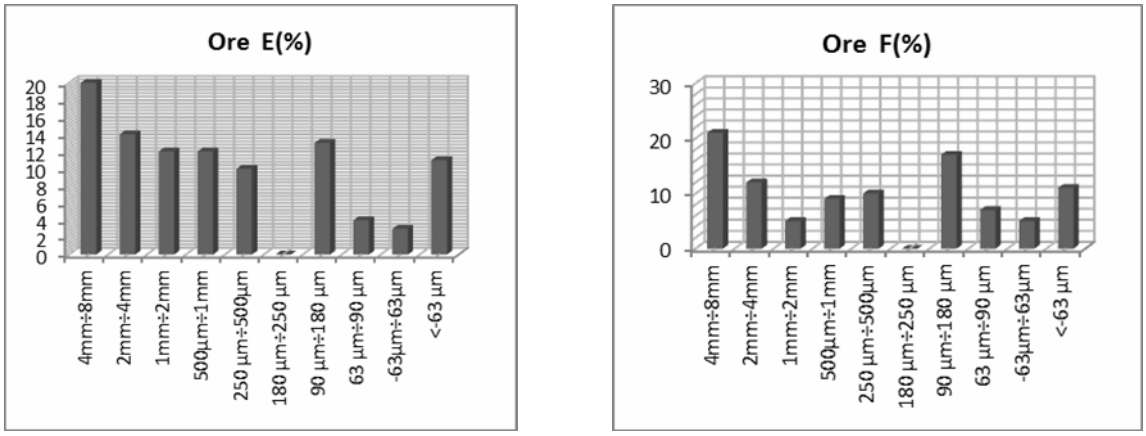


***Fig. 3**. Variation of particle size fraction for each component separately*

### *2.2. Mathematical analysis*

According to Fig. 1, samples A, B, C, D, E, F are fine ore samples. Surfaces of ore samples can be mathematically calculated with formula (1), assuming that most of the sample particles are spheres, as follows:

$$S = 4\pi \cdot n \cdot r^2 \quad (1)$$

where: *S* is the total surface area of all particles of unit mass, *r* is the radius of the particles.

Assuming that in this experiment there will be *i* particles, our formula becomes:

$$S_1 = 4\pi \cdot n_1 \cdot r_1^2 \quad (2)$$

$$S_2 = 4\pi \cdot n_2 \cdot r_2^2 \quad (3)$$

$$S_i = 4\pi \cdot n_i \cdot r_i^2 \quad (4)$$

$$S_{1+2+3+...+i} = 4\pi \sum n_i \cdot r_i^2 \quad (5)$$

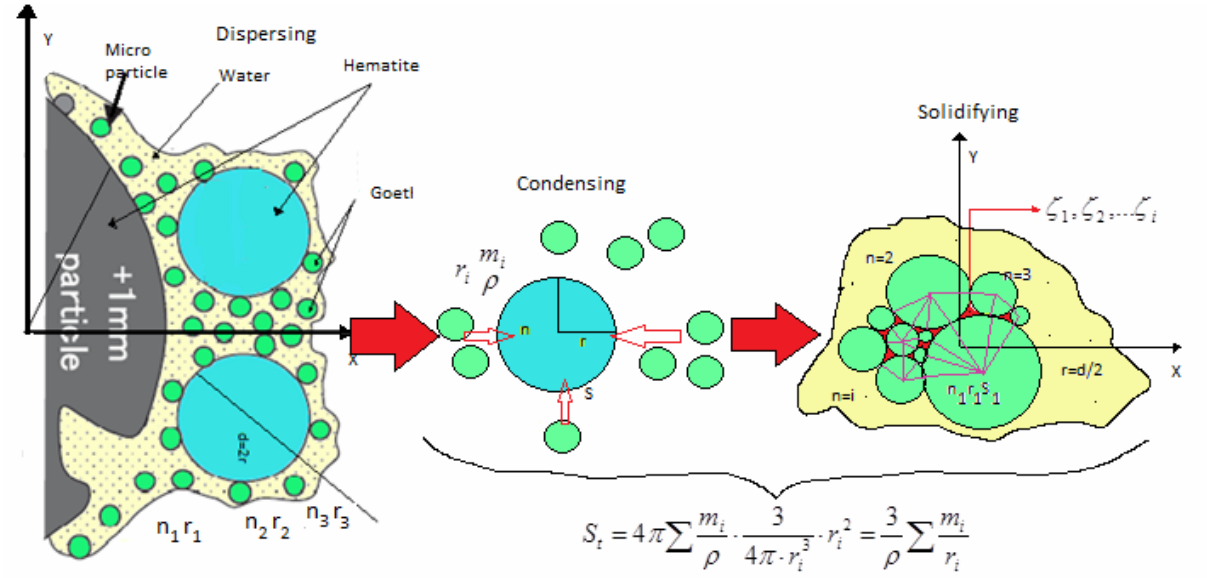


***Fig. 4**. Mathematical calculation of particle diameter*

The total number of particles $n_i$ can be calculated by the relationship:

$$n_i = \frac{m_i}{\rho} \cdot \frac{3}{4\pi \cdot r_i^3}$$

$$S_t = 4\pi \sum \frac{m_i}{\rho} \cdot \frac{3}{4\pi \cdot r_i^3} \cdot r_i^2 = \frac{3}{\rho} \sum \frac{m_i}{r_i}$$

where *m* is the mass of particles of *r* radius compared to a mixture of 100g raw density $\rho$.

We can determine the diameters for each particle. At the same time, with the increase particle diameter, (a fundamental step in preparing sintering), we observe the emergence of a new size ξ-mathematical model imperfections (open spaces), as shown in **Figure 5**.

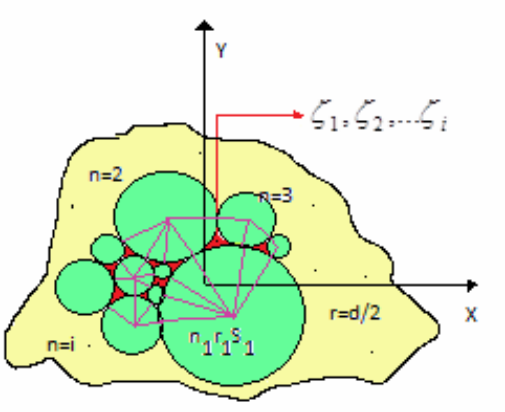


***Fig. 5.*** *Increasing particle diameter*

Here follow relationships depending on particles diameters:

$$\sum r_i^2 = \frac{S_1}{4\pi \cdot n_1} + \frac{S_2}{4\pi \cdot n_2} + \ldots + \frac{S_i}{4\pi \cdot n_i}$$

$$\sum r_i^2 = \frac{1}{4\pi} \sum \frac{S_i}{n_i}$$

$$\sum 4r_i^2 = \frac{1}{\pi} \sum \frac{S_i}{n_i}$$

$$\sum 2r_i = \frac{\sqrt{\pi}}{\pi} \sqrt{\sum \frac{S_i}{n_i}}$$

If we note $d = 2r$, $r \geq 0$, the diameter of each particle; $S_\xi$-surface imperfections, $S_s$-sintering surface, the relationship becomes:

$$\sum d_i = \frac{\sqrt{\pi}}{\pi} \sqrt{\sum \frac{S_i}{n_i}}$$

$$S_s = S_i - S_\zeta$$

Note that with the migration of particles, $\xi \to 0$ (reducing the distances between particles). This is necessary because small diameter spherical particles have a low grip and the sintering process is difficult. This is necessary to obtain particles with large diameters and high porosity mathematical method.

## *2.3. Chemical composition analysis*

The chemical composition of the 6 types of ore is given in **Table 8** and **Figure 6**. In all 6 samples over 50% of the chemical composition is owned by Fe, dominated by raw materials with a low basicity and MgO content between 0.02% -0.05%.

***Table 8.*** *Chemical composition of ores*

| Ch. Composition | Ore A | Ore B | Ore C | Ore D | Ore E | Ore F |
|---|---|---|---|---|---|---|
| Fe | 64.2 | 67.2 | 68.3 | 64.7 | 64.5 | 65.2 |
| $SiO_2$ | 5.1 | 0.6 | 1.3 | 4 | 4.2 | 4.2 |
| $Al_2O_3$ | 1 | 0.94 | 0.9 | 1.1 | 0.7 | 0.8 |
| $TiO_2$ | 0.08 | 0.03 | 0.04 | 0.03 | 0.07 | 0.09 |
| CaO | 0.02 | 0.01 | 0.03 | 0.05 | 0.02 | 0.03 |
| MgO | 0.03 | 0.02 | 0.04 | 0.05 | 0.04 | 0.05 |
| $Na_2O$ | 0.005 | 0.01 | 0.006 | 0.02 | 0.006 | 0.006 |
| $K_2O$ | 0.008 | 0.01 | 0.004 | 0.01 | 0.006 | 0.007 |
| Mn | 0.2 | 0.45 | 0.229 | 0.2 | 0.07 | 0.07 |
| P | 0.045 | 0.037 | 0.03 | 0.04 | 0.057 | 0.04 |
| S | 0.007 | 0.01 | 0.005 | 0.005 | 0.006 | 0.006 |
| V | 0 | 0 | 0.006 | 0 | 0 | 0 |
| LOI | 1.5 | 1.4 | 0.61 | 0.05 | 2.3 | 1.5 |

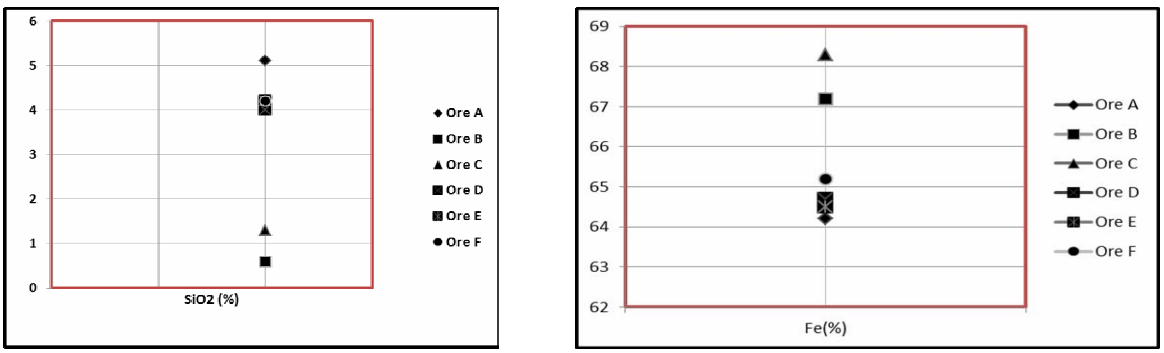


***Fig. 6.*** *Fe and $SiO_2$ distribution in the samples analysed*

Ore C holds a significant amount of iron and ore A, is a low one. We see an inverse distribution in the amount of Fe and $SiO_2$ in that ore, with a high quantity of Fe correspond a small amount of $SiO_2$, ore C with 1.3% $SiO_2$ and 68.3% Fe, respectively ore A with 5.1% SiO2 and 64.2% Fe.

The chemical composition shows that these types of ores can be successfully used in the sintering process. Meet one ore with a $SiO_2$ content <1%, as-$Al_2O_3$ can be used to reduce ores containing $SiO_2$ or in combination with Australian ore, where it prevails, and can be successfully used in Europe and the Far East. P and Mn levels are moderate, and the basic oxides level is very low for these types of ores (MgO and CaO).

The S, V, and other impurities level is very low. The alkalinity level is low, mainly due to the high amount of $SiO_2$ in ores A, D, E and F.

**Table 9 and Figure 7** shows the distribution of alkalinity in the type of ore. Minimum values <0.01 are typical for ore A, E and F, and the maximum for ores C at a rate of CaO/SiO2 = 0.023.

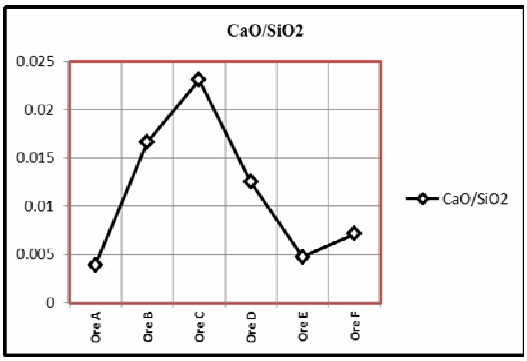


***Fig. 7.*** *Alkalinity evolution depending on the type of ore*

***Table 9.*** *Alkalinity variation*

| Ch. Comp. | Ore A | Ore B | Ore C | Ore D | Ore E | Ore F |
|---|---|---|---|---|---|---|
| CaO/SiO2 | 0.004 | 0.017 | 0.0231 | 0.013 | 0.0048 | 0.007 |
| ΣOa | 5.18 | 0.63 | 1.34 | 4.03 | 4.27 | 4.29 |
| ΣOb | 1.063 | 0.99 | 0.98 | 1.23 | 0.772 | 0.893 |
| ΣEd | 0.007 | 0.01 | 0.011 | 0.005 | 0.006 | 0.006 |
| ΣOb/ΣOa | 0.205 | 1.571 | 0.7313 | 0.305 | 0.1808 | 0.208 |

## 3. Conclusions

The preparation for sintering requires a particle size analysis for quality and high efficiency of processes. Particles with a small diameter can be used for the sintering process after previous training, their measurement can be done by diffraction into developing comparative simulation models needed later to develop the first fusion iron.

The difference between the 2 measurements is that if the mathematical model size $\xi \to 0$ (the spaces between particles shrinks iron ore with small and spherical diameter have low grain capacity), in practical measurements $\xi \neq 0$ because the efficiency of grain increases with the increase of water saturation and iron ore. Size $\xi$ depends on the homogeneity of the particle size, shape, total and initial surface sintering bed.

## References

**[1]. S. N. Ahsan, T. Mukherjee and J. A. Whiteman -** Ironmaking Steelmaking, 10 (1983), 54.
**[2]. N. J. Bristow and C. E. Loo -** ISIJ Int., 32 (1992), 819.
**[3]. T. Maeda and Y. Ono** - Tetsu-to-Hagané, 77 (1991), 1569.
**[4]. Y. H. Yang and N. Standis** - ISIJ Int., 31 (1991), 468.
**[5]. S. C. Panigrahy, P. Verstraeten and J. Dilewinjns** - Metall. Trans. B, 15B (1984), 23.
**[6]. Yu. S. Karabasov, A. N. Pokhvishev, E. F. Shkurko and V. S. Valvin -** Steel USSR, 5 (1975), 583.
**[7]. N. K. Kornilova, E. F. Vegman and S. E. Lazutkin** - Steel USSR, 3 (1973), 1.
**[8]. T. Hamada, T. Koitabashi and K. Okabe -** Tetsu-to-Hagané, 60 (1974), 465.
**[9]. H. Toda and K. Kato** - Trans. Iron Steel Inst. Jpn., 24 (1984), 178.
**[10]. Y. Hosotani, N. Konno, K. Yamaguchi, T. Orimoto and T. Inazumi** - ISIJ Int., 36 (1996), 1439.
**[11]. N. Matsuo, T. Maeda and Y. Ono -** CAMP-ISIJ, 4 (1991), 1081.
**[12]. S. Sato, M. Ichidate, K. Kato and T. Kawaguchi -** Tetsu-to-Hagané, 69 (1983), S744.
**[13]. D. Jeulin, J. L. Latailleur, A. M. Schneider** - Proc. Int. Symp. on Agglomeration (Agg. 77), ed. by K. V. S. Sastry, Amer. Inst.of Mining, Metallurgical & Petroleum Engineers, NY, (1977), 526.
**[14]. Ram Pravesh Bhagat, Uday Shankar Chattoraj** - ISIJ Int., 46 (2006), 1728.
**[15]. Takeshi Maki and Isao Sekiguchi -** ISIJ Int., 49 (2009), 631.
**[16]. Shinji Kawachi and Shunji Kasama** - ISIJ Int., 51 (2011), 1057.
**[17]. Xuewei LV, Xiaobo HUANG, Jaqing YIN** and **Chenguang BAI** - ISIJ Int., 51 (2011), 1432.